
# 3-NP-induced Huntington's-like disease impairs Nrf2 activation without loss of cardiac function in aged rats

A. Silva-Palacios, M. Ostolga-Chavarría, M. Buelna-Chontal, C. Garibay, S. Hernández-Reséndiz, F.J. Roldán, P.L. Flores, A. Luna-López, M. Königsberg, C. Zazueta

PII: S0531-5565(17)30376-5
DOI: doi: 10.1016/j.exger.2017.06.009
Reference: EXG 10074

To appear in: *Experimental Gerontology*

Received date: 10 May 2017
Revised date: 12 June 2017
Accepted date: 13 June 2017

Please cite this article as: A. Silva-Palacios, M. Ostolga-Chavarría, M. Buelna-Chontal, C. Garibay, S. Hernández-Reséndiz, F.J. Roldán, P.L. Flores, A. Luna-López, M. Königsberg, C. Zazueta , 3-NP-induced Huntington's-like disease impairs Nrf2 activation without loss of cardiac function in aged rats, *Experimental Gerontology* (2016), doi: 10.1016/j.exger.2017.06.009

# 3-NP-induced Huntington's-like disease impairs Nrf2 activation without loss of cardiac function in aged rats

A. Silva-Palacios[1, 2, a], M. Ostolga-Chavarría[1], M. Buelna-Chontal[1], C. Garibay[3], S. Hernández-Reséndiz[1], F.J. Roldán[4], P.L. Flores[5], A. Luna-López[6], M. Königsberg[2], C. Zazueta[1&].

[1]Departamento de Biomedicina Cardiovascular, Instituto Nacional de Cardiología, Ignacio Chávez, México

[2]Departamento de Ciencias de la Salud, Universidad Autónoma Metropolitana-Iztapalapa, México

[3]Departamento de Neuropatología, Instituto Nacional de Neurología y Neurocirugía, Manuel Velasco Suárez, México

[4]Departamento de Ecocardiografía, Instituto Nacional de Cardiología, Ignacio Chávez, México.

[5]Departamento de Instrumentación Electromecánica, Instituto Nacional de Cardiología, Ignacio Chávez, México

[6]Departamento de Ciencias Básicas, Instituto Nacional de Geriatría, México

[a]Programa de Posgrado en Biología Experimental, Departamento de Ciencias de la Salud, Universidad Autónoma Metropolitana-Iztapalapa.

[&]Corresponding Author: Cecilia Zazueta

Departamento de Biomedicina Cardiovascular

Instituto Nacional de Cardiología, Ignacio Chávez, México

Juan Badiano No. 1, Sección XVI,

14080, Mexico City, Mexico.

Tel. (+52) 55 5573 2911; Fax. (-52) 55 5573 0926

E-mail address: azazuetam@yahoo.com

**Abstract**

Cardiovascular diseases (CVDs) are one of the leading causes of death in patients over 60 years with Huntington's disease (HD). Here, we investigated if age-related oxidative stress (OS) is a relevant factor to develop cardiac damage in an *in vivo* model of striatal neurodegeneration induced by 3-nitropropionic acid (3-NP). We also evaluated the potential effect of tert-butylhydroquinone (tBHQ) to increase the Nrf2-regulated antioxidant response in hearts from adult and aged rats intoxicated with 3-NP. Our results showed that 3-NP-treatment did not induce cardiac dysfunction, neither in adult nor in aged rats. However, at the cellular level, adult animals showed higher susceptibility to 3-NP-induced damage than aged rats, which suggest that chronic oxidative stress ongoing during aging might have induced an hormetic response that probably prevented from further 3-NP damage. We also found that the oxidative unbalance concurs with unresponsiveness of the Nrf2-mediated antioxidant response in old animals.

146 words

**Key words:** Aging, Nrf2 signaling, 3-Nitropropionic acid, Cardiac function, Hormesis

## 1. Introduction

Current statistics indicate that about 20% of older adults suffer from a neurologic disorder, which means that 400 million people might be potentially affected by neurological diseases in a near future. Huntington's disease (HD) is an inherited genetic disease that occurs in younger patients, but that still shares many features of common neurological diseases prevailing in elderly individuals. It causes loss of medium spiny neurons in the striatal nuclei due to a mutation in the huntingtin gene (Menze et al., 2016). Cognitive and behavioral abnormalities are often accompanied by cardiac dysfunction. In fact, epidemiological studies indicate that cardiovascular diseases prevail in HD patients (Sorensen and Fenger, 1992; Wu et al., 2016) standing for the second-leading mortality cause in HD patients over 60-years old (Lanska et al., 1998; Zielonka et al., 2014; Mielcarek et al., 2014a).

HD transgenic models concur with cardiac dysfunction (Kiriazis et al., 2012; Wood et al., 2012), remodeling processes (Mielcarek et al., 2014a), heart failure (Mihm et al., 2007), diminished hypertrophic response (Mielcarek et al., 2014b), impaired energy imbalance and nucleotide metabolism (Toczek et al., 2016a; Toczek et al., 2016b). Moreover, 3-nitropropionic acid (3-NP) systemic administration, an accepted model that mimics HD symptoms and neuropathology (Hariharan et al., 2014), has been related with histological, biochemical and ultrastructural changes in mice muscle (Gabrielson et al., 2001; Hernández-Echeagaray et al., 2011), along with decrement in blood pressure, bradycardia and ATP diminution in heart atria (Castillo et al., 1993). 3-NP also induces the opening of the mitochondrial permeability transition pore (mPTP) (Mirandola et al., 2010) and inhibits oxygen consumption in isolated cardiac mitochondria (López et al., 1998). It is accepted that 3-NP-induced neurodegeneration relies on the irreversible inhibition of mitochondrial succinate dehydrogenase (SDH) producing an energetic deficit, excitotoxicity and oxidative stress (Liot et al., 2009; Cho and Kim, 2015).

One of the most relevant players in maintaining redox cellular homeostasis is the transcription factor Nrf2 (nuclear E2-related factor 2), which is activated either by reactive oxygen species

(ROS), electrophilic agents (e.g., dimethylfumarates, aldo-keto reductases, oltipraz) or natural compounds (e.g., curcumin, sulforaphane) (Abed et al., 2015; Lu et al., 2016; Penning, 2017). Age-dependent decline in the antioxidant response has been related with reduced nuclear translocation and/or Nrf2 stability loss (Safdar et al., 2010, Miller et al., 2012; Silva-Palacios et al., 2016). However, some reports have shown that several interventions such as exercise training (Gounder et al., 2012), α-lipoic acid (Suh et al., 2004) and tert-butylhydroquinone (tBHQ) treatments (Alarcón-Aguilar et al., 2014) restored Nrf2 nuclear levels or protected cells from further damage (Silva-Palacios et al., 2017) in different models.

Consequently, since cardiac complications associated to HD have not been explored during aging, and neither if attenuation of oxidative stress might be a possible mechanism for cytoprotection, in this work we evaluated if heart dysfunction coexists with 3-NP-induced neurodegeneration and, if the nuclear factor Nrf2 could be pharmacologically activated by tBHQ in old rats.

## 2. Material and Methods

### *2.1 Animals and ethical approval*

Adult (9 months-old) and old (24 months-old) albino Wistar female rats (*Rattus norvegicus*), provided by the closed breeding colonies at the National Institute of Cardiology, Ignacio Chavez and Autonomous Metropolitan University-Iztapalapa were used in this study. A total of 39 adult and 36 old rats were employed. The animals were kept in acrylic boxes under standard conditions of room temperature (25 ± 3°C) and 12h light:12h dark cycles. They were housed 3-per-cage in acrylic boxes and provided with standard commercial rat diet (Rodent Chow; Purina, St. Louis, MO) and water *ad libitum*. All animals were handled according to the criteria established by the standard of "Care and Use of Laboratory Animals" published by the United States National Institutes of Health (US-NIH, NIH publication 85-23, 1985) and approved by the Ethics Committee of the National Institute of Cardiology, Ignacio Chavez. The experimental protocols followed the guidelines of

Official Mexican Standard for the use and care of laboratory animals (NOM-062-ZOO-1999) and for disposal of biological residues (NOM-087-SEMARNAT-SSA1-2002).

### *2.2 Reagents*

Tert-butylhydroquinone (tBHQ), 3-nitropropionic acid (3-NP) and other chemicals were purchased from Sigma-Aldrich (San Luis, MO). The compounds were dissolved in isotonic saline solution (ISS) for subsequent injection. Chemiluminescent detection system and Oxiblot™ kit were obtained from Millipore (Bedford, MA). The kits used for electrophoretic mobility assay (EMSA) and for nuclear protein extraction were purchased from Thermo Scientific (Pierce Biotechnology, Rockford, IL, USA).

### *2.3 Antibodies*

All primary antibodies were obtained from commercial sources and used according to the manufacturer´s recommendations. Anti-Nrf2 (sc-722), anti-GST (sc-138), anti-γ-GCS (sc-22755), anti-glyceraldehyde-3-phosphate dehydrogenase (GAPDH, sc-47724) were obtained from Santa Cruz Biotechnology (Santa Cruz, CA). Anti-HO-1 (#3391) from BioVision (Milpitas, CA), anti-MMP-2 (#13405) from Millipore (Bedford, MA) and anti-Collagen-III (#26310) from GeneTex (San Antonio, TX). Either anti-GAPDH or anti-actin were used as loading control for cytosolic fractions and lamin A (ab26300, Abcam, Cambridge, MA) for nuclear fractions.

### *2.4 Experimental groups*

Adult and elderly rats were randomly assigned into 4 experimental groups as shown in *Figure 1* and described below:

1. *Control group*, rats that received only ISS intraperitoneally (i.p) as vehicle during 11 days.
2. *tBHQ group*, rats received ISS i.p during 4 days and then tBHQ (100 mg/Kg/day) i.p for 7 days.

3. *3-NP group*, rats received ISS i.p for 7 days and then 3-NP (10 mg/Kg/2 doses per day) i.p. for 4 days.
4. *Preconditioned group (PreC),* rats treated with tBHQ i.p. for 7 days, followed by 3-NP treatment (10 mg/Kg/2 doses per day) i.p. for 4 days.

This particular 3-NP-administration protocol has been associated with striatal degeneration and HD symptoms such as increased reactive gliosis, cell death and hypoactive motor behavior. tBHQ-conditioning as described here has been previously reported to diminishes all those conditions (Silva-Palacios et al., 2017).

### *2.5 Evaluation of cardiac function by echocardiography*

Rats from the different groups were anesthetized with a low dose of sodium pentobarbital (1.9 mg/100g body weight, i.p.) to perform echocardiographic analysis using a Sonos 550 echocardiographer (Koninlijke Philips Electronics, Eindhoven, The Netherlands) using a 12 MHz transducer according to our previous report (Hernández-Reséndiz et al., 2013). Paraesternal short and long axis were analyzed by two-dimensional M-mode echocardiography, evaluating at least 3 pulses in each rat. The cavity and the thickness of the left ventricle (LV) were measured to calculate the ejection fraction (EF) using the formula: $\%EF=Y+[(100-Y)\bullet 0.15)$, where $Y=[LVEDD^2-LVESD^2/LVEDD^2]\bullet 100$ as well as the fractional shortening $\%FS=[(LVEDD-LVESD/LVEDD)\bullet 100]$, where LVEDD is the dimension of the LV at the end of diastole, LVESD is the dimension of LV at the end of systole (Stein et al., 2007). Animals were allowed to recover for some days before euthanization.

### *2.6 Histological analysis*

The animals were anesthetized with sodium pentobarbital (5mg/100g body weight, i.p.) and complete lack of pain response was assessed by determining pedal withdrawal reflex. Hearts and

lungs were extracted and weighted. Cardiac tissue was fixed in *p*-formaldehyde 4% for 48 h, embedded in paraffin and serially sectioned on a microtome rotation Leica RM 2125RT (Leica Biosystems, Wetzlar, Germany). Cardiac tissue sections (2 μm thick) were stained with hematoxylin-eosin (H&E) or Masson's trichrome. Left ventricles were analyzed using a Carl Zeiss Primo Star Image Analyzer with an integrated Zeiss Axiocam ERc 5S camera (LLC, US).

### *2.7 Protein carbonylation assay*

Carbonyl groups were detected using the Oxiblot™ Protein Oxidation Detection kit (Millipore, Billerica, MA), according to the manufacture's instructions. Band intensity was digitally quantified using Image Studio Lite Software (Li-Cor Biosciences, Lincoln, Nebraska USA).

### *2.8 Lipid peroxidation assay*

Thiobarbituric acid reactive substances (TBARS) analysis was used to evaluate lipid peroxidation in heart homogenates according to Persky et al. (2000) with some modifications. Cardiac tissue homogenates were heated for 20 min at 37ºC before adding 20% of trichloroacetic acid (TCA) in hydrochloric acid (HCl) 1M. The samples were incubated with 1% thiobarbituric acid (TBA) for 15 min in boiling water (90ºC) and then, placed on ice and centrifuged at 500 × g for 15 min at 4ºC. The formed MDA•TBA adduct in the supernatant was detected at 532 nm in a Beckman DU-65 Spectrophotometer (Brea, California, USA). MDA concentrations were calculated against a standard curve of 1,1,3,3-tetramethoxypropane (TMPO) and results were expressed in TBARs nmol/mg protein. Protein concentration was determined according to Lowry et al. (1951).

### *2.9 Reduced glutathione quantification*

Glutathione determination was made according to Buelna-Chontal et al. (2014). In brief, heart homogenates were incubated in a reaction mixture containing Krebs-Henseleit buffer, pH 7.4, 1 mM monochlorobimane (mCB) and glutathione S-transferase (1 U/ml). Changes in fluorescence

were measured at $\lambda_{ex}$ 385 nm and $\lambda_{em}$ 478 nm in a Perkin Elmer LS 55 Fluorescence Spectrometer (Waltham, Massachusetts, US) at 37ºC. The obtained values were compared with a GSH standard curve and results were expressed as μM GSH/mg protein. Protein concentration was determined according to Lowry et al. (1951).

### *2.10 Cytosolic and nuclear fractions isolation*

Heart tissue (100 mg) was obtained at the end of the experimental protocols. Tissue was frozen and grinded to powder using a mortar and a pestle. Then the pulverized tissue was dissolved in 1 ml of ice cold RIPA lysis buffer (20 mM Tris-HCl, pH 7.5, 150 mM NaCl, 0.1% SDS, 0.5% sodium deoxycholate) and 10 μl phenylmethylsulfonyl fluoride (1 mM) (Hernández-Reséndiz et al., 2015), supplemented with protease inhibitor (Complete™, Mini Protease Inhibitor Cocktail, Roche) and homogenized using a Dounce homogenizer in cold. Homogenates were centrifuged at 11,000 × g for 15 min at 4ºC, the supernatant was transferred in a new tube and stored at -70ºC for further analysis. Cytosolic and nuclear fractions were obtained with the NE-PER® kit (Thermo Scientific, Pierce Biotechnology, Rockford, IL, USA) according to manufacturer´s instructions and stored at -70ºC. Protein concentration was determined according to Lowry et al. (1951).

### *2.11 Western blot analysis*

Proteins (30-50 μg) from each fraction protein were separated on 10-15% SDS-PAGE, transferred to polyvinylidene difluoride (PVDF) membranes (Inmobilon®-P, Millipore Billerica, MA) and incubated with specific primary antibodies against Nrf2 (1:200), GST (1:200), γ-GCS (1:200), HO-1 (0.5μg/ml), MMP-2 (0.5μg/ml) and Collagen-III (1:1000). The immunoblotted proteins were visualized using a chemiluminescent detection system (Millipore Billerica, MA). Each membrane was incubated with their respective load control (markers of cytosolic and/or nuclear fractions, GAPDH/Actin (1:1000) and Lamin-A (1:1000), respectively. All images were analyzed using an Image Studio Lite Software (Li-Cor Biosciences, Lincoln, Nebraska USA).

### *2.12 Electrophoresis mobility assay (EMSA)*

Electrophoresis mobility assay was performed according to Buelna-Chontal et al. (2014). Briefly, biotinylated oligonucleotide containing the antioxidant response element (ARE) sequence (GATCTTTTATGCTGAGTCATGGTTT) (Accesolab S.A. de C.V., Mexico City, Mexico) was used as the DNA target. Nuclear proteins (10 µg) were incubated in binding reaction buffer containing 50 ng/µl poly (dI•dC), 0.05% Nonidet P-40, 2.5% glycerol, 10 mM EDTA, 5 mM $MgCl_2$, 0.05 M KCl and 20 fmol of Biotin-end-labeled ARE (B-ARE) for 60 min at room temperature. The competition assay was performed by adding an excess of unlabeled ARE for 30 min before the addition of B-ARE. Then, the samples were loaded onto native 5% polyacrylamide gel pre-electrophoresed for 60 min in Tris-Borate-EDTA (TBE) buffer. The complexes were separated at 100 V and transferred onto a positively charged nylon membrane in TBE at 380 mA for 30 min. Transferred DNA was crosslinked to the membrane and chemiluminescence detection was performed using stabilized streptavidin–horseradish peroxidase conjugate. Nrf2-DNA binding analysis was performed using an Image Studio Lite Software (Li-Cor Biosciences, Lincoln, Nebraska USA).

### *2.13 Statistical analyses*

The data represent the mean ± standard deviation (SD) of at least 3 independent experiments for each of the experimental protocols in triplicate. Significance levels ($p<0.05$, $p<0.01$, $p<0.001$) were evaluated through an analysis of variance (ANOVA) followed by a post-hoc test for multiple comparisons using the Tukey test (GraphPad Prism version 6.0).

## 3. Results

### *3.1 Cardiac function and structural analysis*

Representative echocardiograms from both age groups are shown in *Figure 2*. Heart weight (HW), body weight (BW), shortening fraction (SF) and heart rate (HR) increased in control old animals ($p<0.01$) (*Table 1*) in comparison with control adult animals; whereas lung weight/body weight (LW/BW) and left ventricle dimension at end-systole (LVSd) decreased in older animals from the control group ($p<0.01$) as compared to adult animals without any treatment.

Echocardiographic data were similar in all adult animals groups (*Table 1*). Conversely, 3-NP and tBHQ treatment in old animals diminished BW, HW and LVSD as compared with their own control group ($p<0.05$, $p<0.01$). Interventricular septum (IVS) thickness and HW decreased in the PreC adult and old animal groups, but none of these changes were reflected in the ejection fraction (EF), an indicator of cardiac performance. Therefore, 3-NP-induced both neurodegeneration and direct toxic effects in the myocardium of old rats, but did not concur with cardiac dysfunction neither in adult nor in aged rats.

### *3.2 Cardiac histology*

As cells may have thresholds for damage accumulation before function is impaired, we explored the effect of 3-NP between both age groups at a cellular level. Cardiac cells morphological analysis was performed after H&E staining. Adult control group heart sections showed a normal cardiomyocytes architecture with centrally placed nuclei (*Figure 3A*), while in the aged control group, cardiac cells were enlarged (*Figure 3B*). However, in both groups the fibers organization was preserved. Hearts from adults or old animals supplemented with tBHQ, did not show any visible changes as compared with their own controls (*Figure 3C and D*), whereas 3-NP-treatment induced a major myofibrils disorganization in adult hearts (*Figure 3E*), than in old rats hearts (*Figure 3F*). Cardiac structure in the adults PreC group was preserved (*Figure 3G*), whereas no obvious changes in aged heart were observed (*Figure 3H*).

The extracellular matrix major components collagens and fibronectin were analyzed with Masson´s trichrome staining. Compared with the adult control group (*Figure 3I*), older animals showed higher interstitial fibrosis (*Figure 3J*). tBHQ treatment induced a slight increase in fibrosis in adult animals (*Figure 3K*) and exacerbated fibrosis in aged rats cardiac tissue (*Figure 3L*). Perivascular fibrosis was also observed in old animals treated with 3-NP (*Figure 3N*). Interestingly, pre-treatment with tBHQ (PreC group) increased fibrosis in old animals (*Figure 3P*), but not in the PreC adult group (*Figure 3O*), which maintained a similar appearance to their own controls.

### *3.3 Cardiac remodeling*

Myocardium extracellular matrix (MEM) damage and loss are important features of cardiac remodeling associated with age. Metalloproteinase-2 (MMP-2) content in its latent (*Figure 4C*) and active forms (*Figure 4D*) were evaluated in all groups. Active MMP-2 basal levels were higher ($p<0.001$) in heart tissue from old control rats (*Figure 4B*) than in control adult rats (*Figure 4A*). The active form increased up to 50% ($p<0.001$) after 3-NP treatment only in adult hearts, but did not decrease with tBHQ-preconditioning.

Since collagen alterations have been related with MEM changes, collagen-III content was also evaluated. As shown *Figures 4A and B,* collagen-III increased ($p<0.001$) in old control hearts in comparison with control adult hearts, thus corroborating that aging heart undergoes fibrotic remodeling. 3-NP-treatment exacerbated up to 10 times collagen-III content in adult hearts (*Figure 4E, p<0.001*), and tBHQ-preconditioning decreased those levels (*Figure 4A, p<0.001*). These results correlated with the myofibrils organization changes observed before (*Figure 3E*). On the other hand 3-NP-treatment increased collagen-III levels by 60% in older animals compared to their own control; this was partially prevented by tBHQ preconditioning (*Figures 4B and E*). These results show that the cardiac response to 3-NP-induced damage and to tBHQ-pretreatment differs among adult and older individuals.

### *3.4 Oxidative stress damage markers*

In order to correlate the previous response with oxidative damage, protein and lipid oxidation, along with GSH levels were determined. *Figure 5A* shows that 3-NP-treatment augmented oxidized proteins ($p<0.01$) and lipid peroxidation (*Figure 5B*, $p<0.001$) in hearts from adult rats, but did not exert any effect on hearts from aged rats (*Figure 5A and 5B*). On the other hand, tBHQ preconditioning produced a slight decrease, although not significant, in the lipid peroxidation of adult hearts in comparison with aged hearts (*Figure 5B*). However, in both aged groups, tBHQ-preconditioning increased significantly protein oxidation (*Figure 5A*). GSH content was lower in control aged hearts than in hearts from control adult animals ($p<0.05$; *Figure 5C*); 3-NP and PreC adult groups hearts had similar GSH values than their age controls, but tBHQ-preconditioning diminished GSH content in hearts from old rats ($p<0.05$) compared to 3-NP-treatment. These results suggest that sustained oxidative stress during the aging process reaches a threshold that cannot be surpassed by 3-NP action.

### *3.5 Nrf2 nuclear translocation*

To determine if the different oxidative stress response stimulated by 3-N-treatment in hearts from adult and elderly rats was related with changes in Nrf2 regulation, we evaluate its expression and localization in nucleus and cytosol under the different treatments. Western blot analysis showed that Nrf2 levels in cardiac homogenates were similar between adult and old animals (*Figures 6A and B*). Nuclear Nrf2 content significantly diminished ($p<0.01$) in the 3-NP adult group as compared with the control and tBHQ adult groups, and was recovered ($p<0.001$) in the PreC group (*Figures 6C and E*). Conversely, only 3-NP augmented Nrf2 levels ($p<0.05$) in the nucleus of aged hearts (*Figures 6D and E*). These results indicate that although Nrf2 expression is maintained during aging, efficient translocation depends on the stimulus. Besides, tBHQ exerts a different regulation in young and in old individuals.

### *3.6 Nrf2-ARE binding efficiency in adult and aged hearts*

Nuclear extracts from adult and aged hearts were used to evaluate Nrf2 binding to ARE (antioxidant response element) under the different experimental conditions (*Figure 7A*). Nrf2-ARE complex decreased in the 3-NP group ($p<0.05$) from adult hearts in comparison with the control and the tBHQ groups *(Figure 7B)*, but was recovered in the PreC group ($p<0.01$) in relation with augmented Nrf2 nuclear translocation (*Figures 6C and E*) and with γ-glutamylcystenyl synthetase (γ-GCS, $p<0.05$) and glutathione S-transferase (GST, $p<0.001$) enhanced expression (*Figures 7C, D and E*). Conversely, Nrf2 binding to its consensus motif decreased in hearts from all old-rats groups, being lower even than in the adult control group *(Figure 7B)*. Therefore, Nrf2 nuclear translocation in old rats hearts is apparently not compromised (*Figures 6D and E*), but the transcription factor did not bind efficiently to its complementary sequence (*Figure 7A*), precluding the up-regulation of major target antioxidant enzymes, e. g. heme-oxygenase-1 (HO-1), GST and γ-GCS (*Figures 7E*).

## 4. Discussion

Although HD is considered primarily a neurological disease, it has been proposed that it may be examined as a systemic disorder (Sassone et al., 2009; Van der Burg et al., 2009), because numerous periphery organs and tissues are affected in these patients (Phan et al., 2009; Mielcarek et al., 2015). Even more, molecular mechanisms related to HD progression have been found not only in brain, but also in several tissues. In this respect, dilated cardiomyopathy has been observed in HD patients at both early and late stages of neuronal degeneration. Accumulation of adenine nucleotide metabolites in the serum of this patients correlated with cardiac dysfunction and impaired nucleotide metabolism in symptomatic HD mice (Toczek et al., 2016a; Toczek et al., 2016b). Other studies have associated HD pathophysiology with increased oxidative stress (Gu et al., 1996; Sapp et al., 1997; Foguem and Kamsu-Foguem, 2016). N-Acetyl-L-Cysteine (NAC) decreases ROS production in cells expressing polyQ and preserves their viability (Vidoni et al., 2016). Indeed,

high lipid peroxidation and low GSH levels in HD patients' plasma have been reported as reliable markers of the progression of this disease (Stoy et al., 2005; Klepac et al., 2007).

Administration of the mitochondrial neurotoxin 3-NP mimics many pathological characteristics in HD. It induces caudate-putamen lesions, increases oxidative stress leading to neuronal loss and reactive gliosis in various animal models like rats (Beal et al., 1993) and primates (Brouillet et al., 1999, Lee and Chang, 2004; Browne and Beal, 2006). The use of 3-NP as a pharmacological model of HD in animals have several advantages; it reproduces the pathophysiology observed in patients (Mehan et al., 2017), it easily cross the blood-brain barrier when administered systemically (Stavrovskaya et al., 2016) and its main action has been related with mitochondrial dysfunction, in particular with complex II inhibition and ROS generation (Liot et al., 2009).

Early studies in young and adult rodents showed that acute 3-NP-treatment promoted cardiac morphological changes, characterized by sarcomere disorganization and fibrosis (Gabrielson et al., 2001), M-bands disruption (Hernández-Echeagaray et al., 2011), along with increased vasodilatation (Castillo et al., 1994) and bradycardia (Hong et al., 1990). Here, we found that 3-NP-treatment induces myofibrils disorganization only in adult hearts (*Figure 3*). Interestingly, heart function was preserved in both age groups (*Table 1*). Discrepancies between the damage observed in the former studies and ours might be due to the higher doses of 3-NP previously used (e.g. 75-100 mg/Kg). However, it is important to specify that in our model, the animals developed HD neurological characteristics related to the late stage of the disease (Silva-Palacios et al., 2017).

At the cellular level, 3-NP-treatment produced oxidative damage in adult heart (*Figure 5*), confirming the concept that stresses and noxious influences exert their effects first at the molecular or biochemical level. Interestingly, such damage was only observed in adult animals but not in aged individuals (*Figure 5*).

Lately hormesis has gained special attention during the aging process (Luna-López et al., 2014). Hormesis is defined as "*a process in which exposure to a low dose of a chemical agent or environmental factor that is damaging at higher doses induces an adaptive beneficial effect on the*

*cell or organism*" (Calabrese and Baldwin, 2003; Rattan, 2006; Calabrese, 2008; Mattson, 2008; Hoffmann, 2009; Calabrese et al., 2010; Holmström and Finkel, 2014). Under certain circumstances, low levels of reactive oxygen species (ROS), which are able to modify redox state, may induce an hormetic response by activating the survival and antioxidant response, that may be beneficial in the long term (Luna-López et al., 2010; Pan et al., 2011; Luna-López et al., 2014). In this sense, our results suggest that an hormetic response might have been established in aged hearts, having undergone sub-chronic oxidative stress throughout life. Sustained oxidative stress and antioxidant response might have reached a threshold that cannot be surpassed by 3-NP action (*Figure 5*). In these regard, Constantini et al. (2014) have proposed that such different an unexpected responses might result from the diverse types and degrees of stress exposure, to the cellular stage at which the stressful environment was experienced, or due to the duration of stressor exposure.

3-NP administration has been associated with impaired mitochondrial function, e. g. mitochondrial membrane potential depolarization (Nasr et al., 2003), cytochrome c release (Antonawich et al., 2002) and ROS production (Liot et al., 2009). Besides the 3-NP specific inhibition of succinate dehydrogenase (Complex II) (Pandey et al., 2008), other mechanisms involved in 3-NP oxidative stress generation involve decreased mitochondrial Complex I (Pandey et al., 2008) and III activities (Orozco-Ibarra et al., 2016). Indeed, it has been proposed that complex II, regulates mitochondrial ROS production through a succinate-dependent interaction with complex I (Zoccarato et al., 2009; 2011). Furthermore, *in vitro* studies have shown that in the presence of 3-NP, mitochondria generate superoxide from a site located between the ubiquinol pool and 3-NP-binding site in complex I (Bacsic et al., 2006).

On the other hand, Meng et al., (2017) recently proposed a new concept called redox-stress response capacity (RRC) to describe cells ability to respond to oxidative stress; specifically to generate a dynamic response to maintain cellular redox homeostasis. Oxidative stress is considered a main feature during the natural aging process and a unifying mechanism in age-related

pathologies (Silva-Palacios, 2016); however, some researchers have found that oxidants might have a positive effect on regulating life expectancy (Rodriguez et al., 2011) or at least, that increased ROS do not accelerates the aging process (van Remmen et al., 2003). It has also been suggested that oxidative stress effect in aging depends on specific environments or on particular stimulus (Salmon et al., 2010), and that under specific conditions the antioxidant genes transcriptional regulation might be regulated. Nrf2 has been recognized as the antioxidant response master transcriptional regulator and its loss or deregulation is associated with several pathologies and aging (Kumar et al., 2016). Controversial data exist on the mechanisms that lead to Nrf2 dysfunction in aged organisms, including inactivation of the factor in the cytosol, failure in its nuclear translocation or dysfunction on downstream gene expression mechanisms (Silva-Palacios et al., 2016). In this regard, a recent study reports that Nrf2 nuclear import is impaired in elderly patients (Gounder et al., 2012). Others studies have determined that nuclear Nrf2 levels in aged rats subjected to moderate exercise, reach comparable values to those observed in young mice (Done et al., 2016) and that α-lipoic acid administration to old rats activates nuclear Nrf2 translocation (Suh et al., 2004). Our results add evidence to the proposal that Nrf2 activation pathway might remain intact in old animals (*Figure 7*), since we did not find differences between nuclear Nrf2 levels in hearts from adult or aged rats (*Figure 6*).

Thus, the hormetic response observed in the aged rats might fit into the redox-stress response capacity (RRC) concept recently described (Meng et al., 2017). Indeed, our findings highlight the priority studying Nrf2 activators as a reliable therapy to treat age-related diseases and makes mandatory to find the missing links in Nrf2 signaling and regulation during this life stage.

## 5. Conclusion

3-NP exerts differential effects in cardiac tissue depending on age. The lack of effects observed in old animals might be related to a previously gained hormetic response in which the threshold for oxidative damage was reached and could not be surpassed in old animals. Our data showed that the

antioxidant response Nrf2 is functional in adult animals, but it is compromised in old animals (*Figure 8*), possibly due to deregulation of Nrf2 signaling cascade downstream components.

## 6. Acknowledgments

This article is part of the doctoral thesis of Alejandro Silva-Palacios in the Experimental Biology Doctoral Program, Autonomous Metropolitan University, Campus Iztapalapa. Alejandro Silva-Palacios received a scholarship from the National Council of Science and Technology (CONACyT) and this work was partially supported by Grants 177527 to CZ and FON.INST/298/2016 to MK from CONACyT, Mexico. The authors thank Dr. A. Hernández from CINVESTAV for generously donating us the actin antibody.

## 7. References


1. Abed DA, Goldstein M, Albanyan H, Jin H, Hu L, 2015. Discovery of direct inhibitors of Keap1-Nrf2 protein-protein interaction as potential therapeutic and preventive agents. Acta Pharm Sin B. 5,285-99
2. Alarcón-Aguilar A, Luna-López A, Ventura-Gallegos JL, Lazzarini R, Galván-Arzate S, González-Puertos VY, Morán J, Santamaría A, Königsberg M, 2014. Primary cultured astrocytes from old rats are capable to activate the Nrf2 response against $MPP^+$ toxicity after tBHQ pretreatment. Neurobiol Aging. 35,1901-1912.
3. Antonawich FJ, Fiore-Marasa SM, Parker CP, 2002. Modulation of apoptotic regulatory proteins and early activation of cytochrome C following systemic 3-nitropropionic acid administration. Brain Res Bull. 57,647-649
4. Bacsi A, Woodberry M, Widger W, Papaconstantinou J, Mitra S, Peterson JW, Boldogh I, 2006. Localization of superoxide anion production to mitochondrial electron transport chain in 3-NPA-treated cells. Mitochondrion. 6,235-244
5. Beal MF, Brouillet E, Jenkins BG, Ferrante RJ, Kowall NW, Miller JM, Storey E, Srivastava R, Rosen BR, Hyman BT, 1993. Neurochemical and histological characterization of striatal excitotoxic lesiones produced by the mitochondrial toxin 3-nitropropionic acid. J Neurosci. 13,4181-4192
6. Brouillet E, Condé F, Beal MF, Hantraye P, 1999. Replicating Huntington´s disease phenotype in experimental animals. Prog Neurobiol. 59,427-468
7. Browne SE, Beal MF, 2006. Oxidative damage in Huntington's disease pathogenesis. Antioxid Redox Signal. 8,2061-73
8. Buelna-Chontal M, Guevara-Chávez JG, Silva-Palacios A, Medina-Campos ON, Pedraza-Chaverrí J, Zazueta C, 2014. Nrf2-regulated antioxidant response is activated by protein kinase C in postconditioned rat hearts. Free Radic Biol Med. 74,145-56

9. Calabrese EJ, 2008. Converging concepts: adaptive response, preconditioning, and the Yerkes-Dodson law are manifestations of hormesis. J Ageing Res Rev 7,8–20
10. Calabrese EJ, Baldwin LA, 2003. Hormesis at the National Toxicology Program (NTP): evidence of hormetic dose responses in NTP doserange studies. Nonlinear Biol Toxicol Med 1,455–467
11. Calabrese V, Cornelius C, Mancuso C, Lentile R, Stella AM, Butterfield DA, 2010. Redox homeostasis and cellular stress response in aging and neurodegeneration. Methods Mol Biol 610,285–308
12. Castillo C, Reyes G, Rosas-Lezama MA, Valencia I, Hong E, 1994. Analysis of the cardiodepressor action of 3-nitropropionic acid. Proc West Pharmacol Soc. 37,41-42
13. Castillo C, Valencia I, Reyes G, Hong E, 1993. 3-Nitropropionic acid, obtained from *Astragalus* species has vasodilator and hypotensive properties. Drug Dev. Res. 28,183-188
14. Cho KJ, Kim GW, 2015. Differential caspase activity in the cortex and striatum with chronic infusion of 3-nitropropionic acid. Biochem Biophys Res Commun. 465,631-637
15. Costantini D, Monaghan P, Metcalfe NB, 2014. Prior hormetic priming is costly under environmental mismatch. Biol Lett. 10,20131010
16. Done AJ, Gage MJ, Nieto NC, Traustadóttir T, 2016. Exercise-induced Nrf2-signaling is impaired in aging. Free Radic Biol Med. 96,130-138.
17. Foguem C, Kamsu-Foguem B, 2016. Neurodegeneration in tauopathies and synucleinopathies. Rev Neurol (Paris). 172,709-714
18. Gabrielson KL, Hogue BA, Bohr VA, Cardounel AJ, Nakajima W, Kofler J, Zweier JL, Rodriguez ER, Martin LJ, de Souza-Pinto NC, Bressler J, 2001. Mitochondrial toxin 3-nitropropionic acid induces cardiac and neurotoxicity differentially in mice. Am J Pathol. 159,1507-1520
19. Gounder SS, Kannan S, Devadoss D, Miller CJ, Whitehead KJ, Odelberg SJ, Firpo MA, Paine R 3rd, Hoidal JR, Abel ED, Rajasekaran NS, 2012. Impaired transcriptional activity of Nrf2 in

age-related myocardial oxidative stress is reversible by moderate exercise training. PLoS One. 7,e45697

20. Gu M, Gash MT, Mann VM, Javoy-Agid F, Cooper JM, Schapira AH, 1996. Mitochondrial defect in Huntington's disease caudate nucleus. Ann Neurol. 39,385-89
21. Hariharan A, Shetty S, Shirole T, Jagtap AG, 2014. Potential of protease inhibitor in 3-nitropropionic acid induced Huntington's disease like symptoms: mitochondrial dysfunction and neurodegeneration. Neurotoxicology. 45,139-148
22. Hernández-Echeagaray E, González N, Ruelas A, Mendoza E, Rodríguez-Martínez E, Antuna-Bizarro R, 2011. Low doses of 3-nitropropionic acid in vivo induce damage in mouse skeletal muscle. Neurol Sci. 32,241-54
23. Hernández-Reséndiz S, Palma-Flores C, De Los Santos S, Román-Anguiano NG, Flores M, de la Peña A, Flores PL, Fernández-G JM, Coral-Vázquez RM, Zazueta C, 2015. Reduction of no-reflow and reperfusion injury with the synthetic 17β-aminoestrogen compound Prolame is associated with PI3K/Akt/eNOS signaling cascade. Basic Res Cardiol. 110,1-12
24. Hernández-Reséndiz S, Roldán FJ, Correa F, Martínez-Abundis E, Osorio-Valencia G, Ruíz-de-Jesús O, Alexánderson-Rosas E, Vigueras RM, Franco M, Zazueta C, 2013. Postconditioning protects against reperfusion injury in hypertensive dilated cardiomyopathy by activating MEK/ERK1/2 signaling. J Card Fail. 19, 135-146
25. Hoffmann GR, 2009. A perspective on the scientific, philosophical, and policy dimensions of hormesis. Dose Response 7,1–51
26. Holmström KM, Finkel T, 2014. Cellular mechanisms and physiological consequences of redox-dependent signaling. Nat Rev Mol Cell Biol. 15,411-421
27. Hong E, Castillo C, Rivero I, Somanathan R, 1990. Vasodilator and antihypertensive actions of 3-nitropropionic acid. Proc West Pharmacol Soc. 33,209-211

28. Kiriazis H, Jennings NL, Davern P, Lambert G, Su Y, Pang T, Du X, La Greca L, Head GA, Hannan AJ, Du XJ, 2012. Neurocardiac dysregulation and neurogenic arrhythmias in a transgenic mouse model of Huntington's disease. J Physiol. 590,5845-5860

29. Klepac N, Relja M, Klepac R, Hecimovic S, Babic T, Trkulja V, 2007. Oxidative stress parameters in plasma of Huntington's disease patients, asymptomatic Huntington's disease gene carriers and healthy subjects: a cross-sectional study. J Neurol. 254,1676–1683

30. Kumar RR, Narasimhan M, Shanmugam G, Hong J, Devarajan A, Palaniappan S, Zhang J, Halade GV, Darley-Usmar VM, Hoidal JR, Rajasekaran NS, 2016. Abrogation of Nrf2 impairs antioxidant signaling and promotes atrial hypertrophy in response to high-intensity exercise stress. J Transl Med. 14:86

31. Lanska DJ, Lavine L, Lanska MJ, Schoenberg BS, 1998. Huntington's disease mortality in the United States. Neurology. 38,769-772

32. Lee WT, Chang C, 2004. Magnetic resonance imaging and spectroscopy in assessing 3-nitropropionic acid-induced brain lesions: an animal model of Huntington's disease. Prog Neurobiol. 72,87-110

33. Liot G, Bossy B, Lubitz S, Kushnareva Y, Sejbuk N, Bossy-Wetzel E, 2009. Complex II inhibition by 3-NP causes mitochondrial fragmentation and neuronal cell death via an NMDA- and ROS-dependent pathway. Cell Death Differ. 16,899-909

34. Lopez PS, Castillo CH, Pastelín GH, Hernández MR, Suárez MJ, Sánchez ML, Escalante BA, 1998. Characterization of 3-nitropropionic acid-induced bradycardia in isolated atria. Toxicol Appl Pharmacol. 148,1-6

35. Lowry OH, Rosebrough NJ, Farr AL, Randall RJ, 1951. Protein measurement with the Folin phenol reagent. J Biol Chem. 193,265-275

36. Lu MC, Ji JA, Jiang ZY, You QD, 2016. The Keap1-Nrf2-ARE pathways as a potential preventive and therapeutic target: An update. Med Res Rev. 36,924-63

37. Luna-López A, González-Puertos VY, López-Diazguerrero NE, Königsberg M, 2014. New considerations on hormetic response against oxidative stress. J Cell Commun Signal. 8,323-331

38. Luna-López A, Triana-Martínez F, López-Diazguerrero NE, Ventura-Gallegos JL, Gutiérrez-Ruiz MC, Damián-Matsumura P, Zentella A, Gómez-Quiroz LE, Königsberg M, 2010. Bcl-2 sustains hormetic response by inducing Nrf-2 nuclear translocation in L929 mouse fibroblasts. Free Radic Biol Med. 49,1192-1204

39. Mattson MP, 2008. Hormesis and disease resistance: activation of cellular stress response pathways. Hum Exp Toxicol 27,155–162

40. Mehan S, Parveen S, Kaur G, Kukkar U, Dudi R, Rajput M, Kalra S, 2017. Targeting Phytochemical Driver in AC/cAMP/PKA/CREB Activation: The Next Frontier for Alleviating Huntington's Type Neurodegenerative Disorders in 3-NP Animal Model: A Complete Review. EC Neurology 6.3,77-131

41. Meng J, Lv Z, Qiao X, Li X, Li Y, Zhang Y[1], Chen C, 2017. The decay of Redox-stress Response Capacity is a substantive characteristic of aging: Revising the redox theory of aging. Redox Biol. 11,365-374

42. Menze ET, Esmat A, Tadros MG, Khalifa AE, Abdel-Naim AB, 2016. Genistein improves sensorimotor gating: Mechanisms related to its neuroprotective effects on the striatum. Neuropharmacology. 105,35-46

43. Mielcarek M, Inuabasi L, Bondulich MK, Muller T, Osborne GF, Franklin SA, Smith DL, Neueder A, Rosinski J, Rattray I, Protti A, Bates GP, 2014a. Dysfunction of the CNS-heart axis in mouse models of Huntington's disease. PLoS Genet. 10,e1004550

44. Mielcarek M, Bondulich MK, Inuabasi L, Franklin SA, Muller T, Bates GP, 2014b. The Huntington´s disease-related cardiomyopathy prevents a hypertrophic response in the R6/2 mouse model. PLoS One. 9,e108961

45. Mihm MJ, Amann DM, Schanbacher BL, Altschuld RA, Bauer JA, Hoyt KR, 2007. Cardiac dysfunction in the R6/2 mouse model of Huntington's disease. Neurobiol Dis. 25,297-308

46. Mirandola SR, Melo DR, Saito A, Castilho RF, 2010. 3-nitropropionic acid-induced mitochondrial permeability transition: comparative study of mitochondria from different tissues and brain regions. J Neurosci Res. 88,630-639

47. Nasr P, Gursahani HI, Pang Z, Bondada V, Lee J, Hadley RW, Geddes JW, 2003. Influence of cytosolic and mitochondrial $Ca^{2+}$, ATP, mitochondrial membrane potential, and calpain activity on the mechanism of neuron death induced by 3-nitropropionic acid. Neurochem Int. 43,89-99

48. Orozco-Ibarra M, García-Morales J, Calvo-Silva FJ, Fernández-Valverde F, Serrano-García N, 2016. Striatal mitochondria response to 3-nitropropionic acid and fish oil treatment. Nutr Neurosci. 28,1-11

49. Pan Y, Schroeder EA, Ocampo A, Barrientos A, Shadel GS, 2011. Regulation of yeast chronological life span by TORC1 via adapatative mitochondrial ROS signaling. Cell Metab. 13,668-678

50. Pandey M, Varghese M, Sindhu KM, Sreetama S, Navneet AK, Mohanakumar KP, Usha R, 2008. Mitochondrial $NAD^{+}$-linked state 3 respiration and complex-I activity are compromised in the cerebral cortex of 3-nitropropionic acid-induced rat model of Huntington's disease. J Neurochem. 104,420-34

51. Phan J, Hickey MA, Zhang P, Chesselet MF, Reue K, 2009. Adipose tissue dysfunction tracks disease progression in two Huntington's disease mouse models. Hum Mol Genet 18,1006–16

52. Penning TM, 2017. Aldo-keto reductase regulation by the Nrf2 system: Implications for stress response, chemotherapy drug resistance, and carcinogenesis. Chem Res Toxicol. 30,162-76

53. Persky AM, Green PS, Stubley L, Howell CO, Zaulyanov L, Brazeau GA, Simpkins JW, 2000. Protective effect of estrogens against oxidative damage to heart and skeletal muscle in vivo and in vitro. Proc Soc Exp Biol Med. 223,59-66

54. Rattan SI, 2006. Hormetic modulation of aging and longevity by mild heat stress. Dose Response 3,533–546

55. Rodriguez KA, Wywial E, Perez VI, Lambert AJ, Edrey YH, Lewis KN, Lindsey ML, Brand MD, Buffenstein R, 2011. Walking the oxidative stress tightrope: a perspective from the naked mole-rat, the longest-living rodent. Curr Pharm Des. 17, 2290-2307.

56. Safdar A, deBeer J, Tarnopolsky MA, 2010. Dysfunctional Nrf2-Keap1 redox signaling in skeletal muscle of the sedentary old. Free Radic Biol Med. 49,1487-1493

57. Salmon AB, Richardson A, Pérez VI, 2010. Update on the oxidative stress theory of aging: does oxidative stress play a role in aging or healthy aging? Free Radic Biol Med, 48,642-655

58. Sapp E, Schwarz C, Chase K, Bhide PG, Young AB, Penney J, Vonsattel JP, Aronin N, DiFiglia M, 1997. Huntingtin localization in brains of normal and Huntington's disease patients. Ann Neurol. 42,604-12

59. Sassone J, Colciago C, Cislaghi G, Silani V, Ciammola A, 2009. Huntington's disease: the current state of research with peripheral tissues. Exp Neurol. 219,385-97

60. Silva-Palacios A, Königsberg M, Zazueta C, 2016. Nrf2 signaling and redox homeostasis in the aging heart: A potential target to prevent cardiovascular diseases? Ageing Res Rev. 6,81-95

61. Silva-Palacios A, Colín-González AL, López-Cervantes SP, Zazueta C, Luna-López A, Santamaría A, Königsberg M, 2017. Tert-buthylhydroquinone pre-conditioning exerts dual effects in old female rats exposed to 3-nitropropionic acid. Redox Biol. 12,610-624

62. Sorensen SA, Fenger K, 1992. Causes of death in patients with Huntington's disease and in unaffected first degree relatives. J Med Genet. 29,911-914

63. Stavrovskaya AV, Voronkov DN, Yamshchikova NG, Ol'shanskiy AS, Khudoerkov RM, Illarioshkin SN, 2016. Experience of Experimental Modelling of Huntington's Disease. Hum Physiol. 42,898-904

64. Stein AB, Tiwari S, Thomas P, Hunt G, Levent C, Stoddard MF, Tang XL, Bolli R, Dawn B, 2007. Effects of anesthesia on echocardiographic assessment of left ventricular structure and function in rats. Basic Res Cardiol. 102,28-41

65. Stoy N, Mackay GM, Forrest CM, Christofides J, Egerton M, Stone TW, Darlington LG, 2005. Tryptophan metabolism and oxidative stress in patients with Huntington's disease. J Neurochem 93,611–623

66. Suh JH, Shenvi SV, Dixon BM, Liu H, Jaiswal AK, Liu RM, Hagen TM, 2004. Decline in transcriptional activity of Nrf2 causes age-related loss of glutathione synthesis, which is reversible with lipoic acid. Proc Natl Acad Sci U S A. 101,3381-3386

67. Toczek M, Kutryb-Zajac B, Zukowska P, Slominska EM, Isalan M, Mielcarek M, Smolenski RT, 2016a. Changes in cardiac nucleotide metabolism in Huntington´s disease. Nucleosides Nucleotides Nucleic Acids.35,707-12

68. Toczek M, Zielonka D, Zukowska P, Marcinkowski JT, Slominska E, Isalan M, Smolenski RT, Mielcarek M, 2016b. An impaired metabolism of nucleotides underpins a novel mechanism of cardiac remodeling leading to Huntington´s disease related cardiomyopathy. Biochim Biophys Acta. 1862,2147-57

69. Van der Burg JM, Björkqvist M, Brundin P, 2009. Beyond the brain: widespread pathology in Huntington's disease. Lancet Neurol. 8,765-74

70. Van Remmen H, Ikeno Y, Hamilton M, Pahlavani M, Wolf N, Thorpe SR, Alderson NL, Baynes JW, Epstein CJ, Huang TT, Nelson J, Strong R, Richardson A, 2003. Life-long reduction in MnSOD activity results in increased DNA damage and higher incidence of cancer but does not accelerate aging. Physiol Genomics. 16, 29-37

71. Vidoni C, Castiglioni A, Seca C, Secomandi E, Melone MA, Isidoro C, 2016. Dopamine exacerbates mutant Huntingtin toxicity via oxidative-mediated inhibition of autophagy in SH-SY5Y neuroblastoma cells: Beneficial effects of anti-oxidant therapeutics. Neurochem Int. 101,132-143

72. Wood NI, Sawiak SJ, Buonincontri G, Niu Y, Kane AD, Carpenter TA, Giussani DA, Morton AJ, 2012. Direct evidence of progressive cardiac dysfunction in a transgenic mouse model of Huntington's disease. J Huntingtons Dis. 1,57-64

73. Wu BT, Chiang MC, Tasi CY, Kuo CH, Shyu WC, Kao CL, Huang CY, Lee SD, 2016. Cardiac Fas-dependent and mitochondria-dependent apoptotic pathways in a transgenic mouse model of Huntington's disease. Cardiovasc Toxicol. 16,111-121

74. Zielonka D, Piotrowska I, Mielcarek M, 2014. Cardiac dysfunction in Huntington´s disease. Exp Clin Cardiol. 20,2547-54

75. Zoccarato F, Cavallini L, Alexandre A, 2009. Succinate is the controller of $O_2^{\cdot-}/H_2O_2$ release at mitochondrial complex I : negative modulation by malate, positive by cyanide. J Bioenerg Biomembr. 41,387-93

76. Zoccarato F, Miotto C, Cavallini L, Alexandre A, 2011. The control of mitochondrial succinate-dependent $H_2O_2$ production. J Bioenerg Biomembr. 43,359-66

## 8. Figure Legends

**Figure 1. Scheme of treatments administrated to adults and older animals.** Ct: Control group; ISS: isotonic saline solution.

**Figure 2. Effect of 3-NP treatment on cardiac function in adult and old animals**. Representative echocardiographic images (Echo). IVS, interventricular septum; left ventricular dimension in end-diastole (red arrow); left ventricular dimension in end-systole (yellow arrow).

**Figure 3. Left ventricular cross-sections stained with H&E and Masson´s trichrome**. Morphological changes of left ventricle were analyzed by light microscopy (Bars = 40x) in adult and old animals. Images are representative of at least three independent experiments for each group.

**Figure 4. Cardiac remodeling in hearts from adult and old animals.** Representative Western blot images of metalloproteinase-2 (MMP-2) and collagen-III content in (**A**) adult and (**B**) old animals, normalized with GAPDH. (**C)** Densitometric analysis of the signal intensity obtained after chemiluminescent detection. The results were obtained from 3-4 independent experiments and the data are expressed as mean ± SD, $^{a}p<0.001$ *vs.* Ct, $^{b}p<0.01$, $^{c}p<0.001$, $^{d}p<0.05$ *vs*. 3-NP. The asterisks (*) indicate $p<0.001$ *vs.* Adult Ct.

**Figure 5. Markers of oxidative stress damage. (A)** Evaluation of oxidized proteins in cardiac tissue homogenates. For adult animals, $^{a}p<0.05$, $^{b}p<0.01$, $^{c}p<0.001$ *vs.* Ct. For old animals, $^{d}p<0.05$ *vs.* Ct. (**B)** TBARS in cardiac tissue homogenates, $^{a}p<0.001$ *vs* Ct. (**C**) GSH content. For adult animals $^{a}p<0.05$ *vs.* Ct and for old animals $^{b}p<0.05$ *vs.* 3-NP. Data represent the mean ± SD of 4 independent experiments for each group. *$p<0.01$, **$p<0.001$ *vs.* Adult Ct.

**Figure 6. Nrf2 in homogenates, cytosol and nucleus from adult and aged hearts.** Western blot images (**A**) and densitometric analysis (**B**) of Nrf2 content in total homogenates. Nrf2 content in nuclear (Nuc Fra) and cytosolic fractions (Cyt Fra) from adult animals (**C**) and from old animals (**D**). Densitometric analysis of Nrf2 content in Nuc Fra and Cyt Fra from adult and old animals (**E**). Results represent the mean ± SD of 3-4 independent experiments from each group. [a]*p<0.05,* [b]*p<0.01 vs.* Ct, [c]*p<0.001 vs.* 3-NP.

**Figure 7. Nrf2 activation and oxidative response in adult and old animals. (A)** Representative autoradiograph of electrophoretic mobility-shift assay from adult and old hearts. The lanes represent: 1) Control, 2) tBHQ, 3) 3-NP and 4) PreC groups. (**B**) Image analysis of Nrf2-DNA binding obtained by densitometry. Results represent mean ± SD of 3-4 independent experiments in each group. For adult animals [a]*p<0.05 vs. Ct,* [b]*p<0.01 vs. 3-NP and* [c]*p<0.001 vs.* 3-NP for old animals. **p<0.001 vs. Adult Ct.* The Antioxidant enzymes content in adult (**C**) and in old (**D**) animals. (**E)** Densitometric analysis of antioxidant enzymes levels in adult and old animals. Results represent the mean ± SD of 3-4 independent experiments in each group. [a]*p<0.05,* [b]*p<0.001 vs.* Ct, [c]*p<0.01 vs.* 3-NP.

**Figure 8. 3-NP exerts differential effects in cardiac tissue depending on age.** 3-NP induces cellular redox imbalance due to the increase of mitochondrial ROS secondary to Complex II inhibition in heart tissue from adults animals. Conversely, the cells from old animals maintain a pro-oxidant environment, with is not modified by the neurotoxin. In adult cells, Nrf2 is activated by tBQ, the oxidized product of tBHQ which induces the dissociation of Keap1/Nrf2 complex. Subsequent translocation and nuclear activation of Nrf2, correlated with increased antioxidant enzymes such as GST and γ-GSC in adults; while the activation of Nrf2 is compromised in old animals. ROS, reactive oxygen species; GST, glutathione S-transferase; γ -GSC, gamma-glutamyl-cysteine-synthetase; HO-1, heme-oxygenase-1; tBQ, tert-butylbenzoquinone; $O_2$·-, superoxide anion

(blue ovals); $H_2O_2$, hydrogen peroxide (red ovals); Cys, cysteine; Maf, muscle aponeurotic fibrosarcoma; ARE/EpRE, antioxidant response element/electrophiles.

**Table 1. Structural and functional parameters from adult and old animals.** Data are the mean ± SD of at least 3 different animals in each experimental group. The bold numbers indicate *p<0.01 vs.* Ct Adult. [a]*p<0.05*, [b]*p<0.01 vs.* its own Ct.

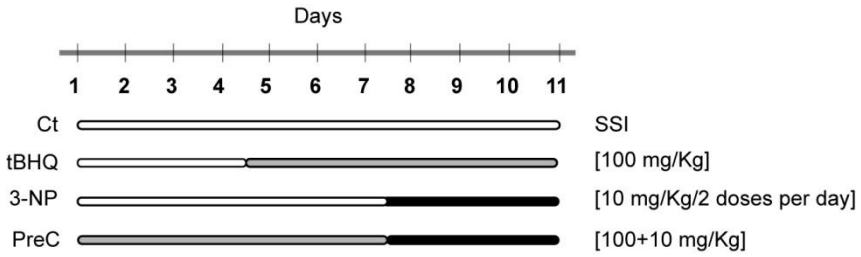


Fig. 1

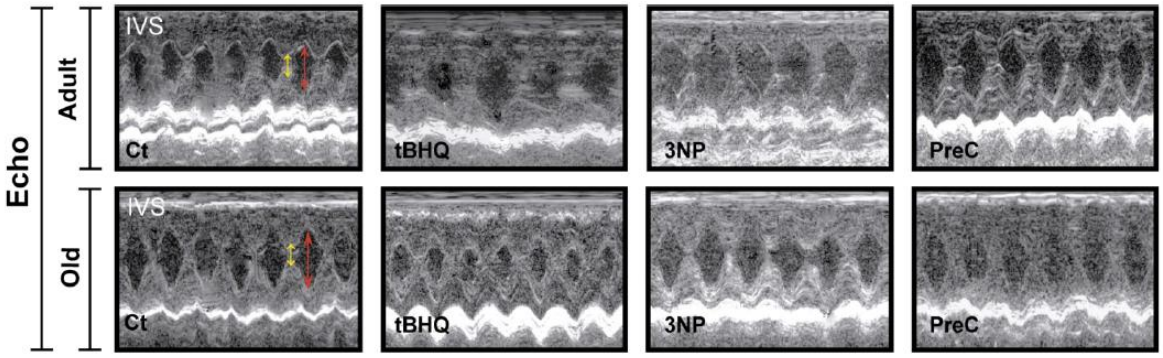


Fig. 2

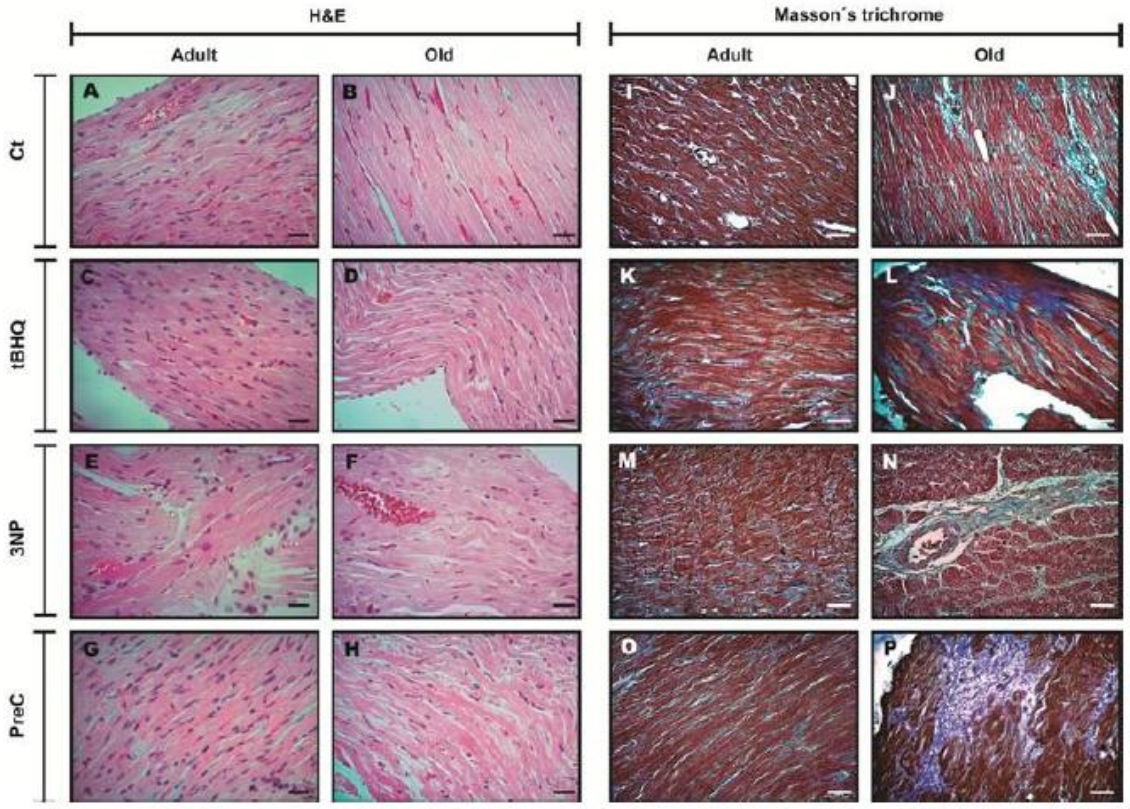


Fig. 3

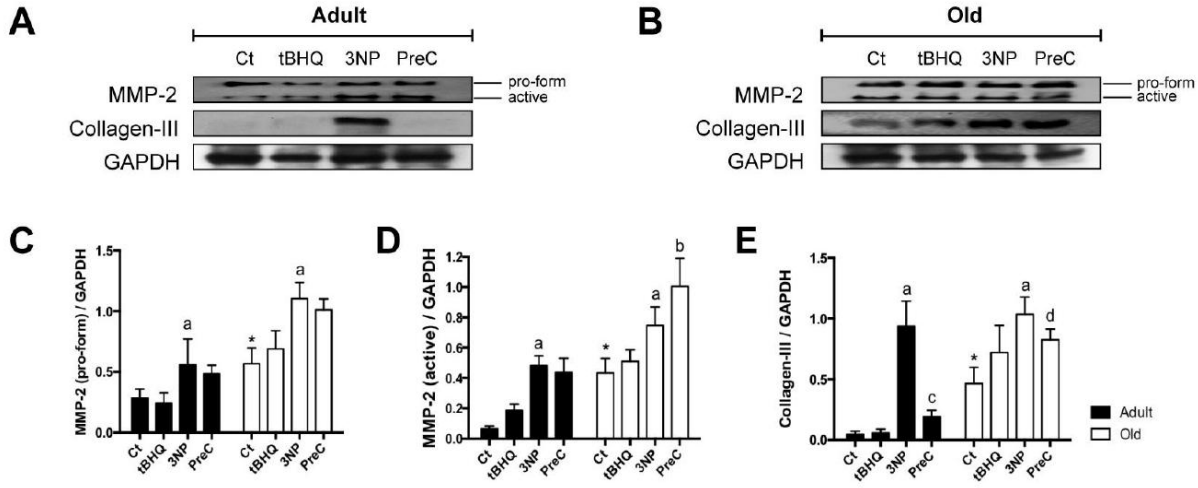


Fig. 4

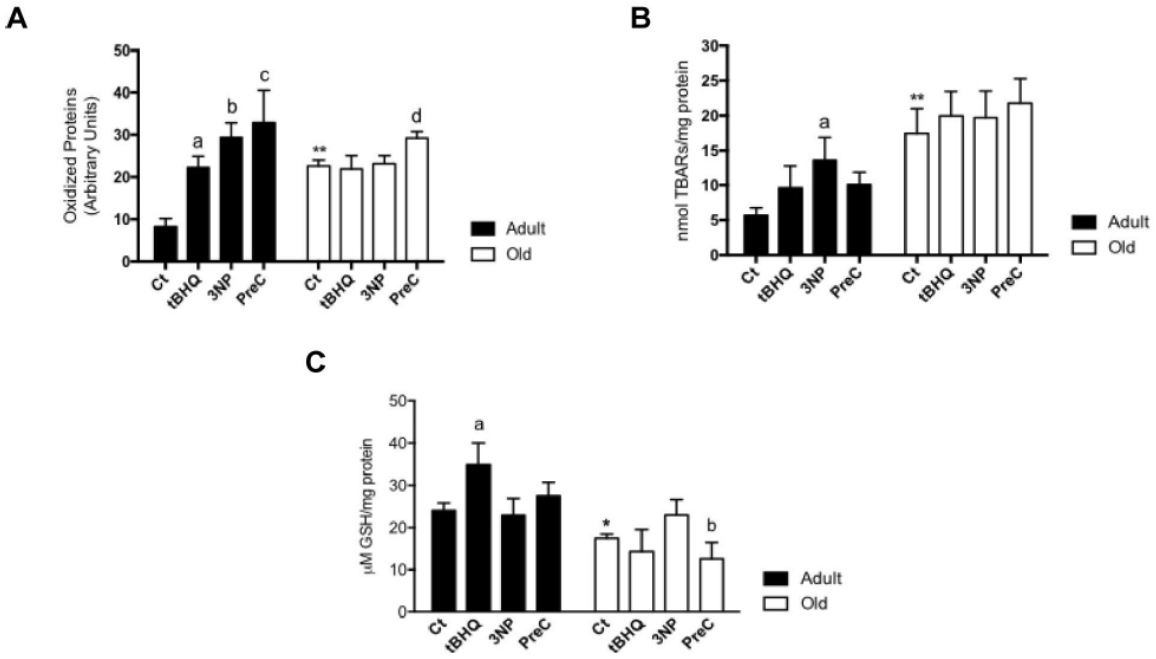


Fig. 5

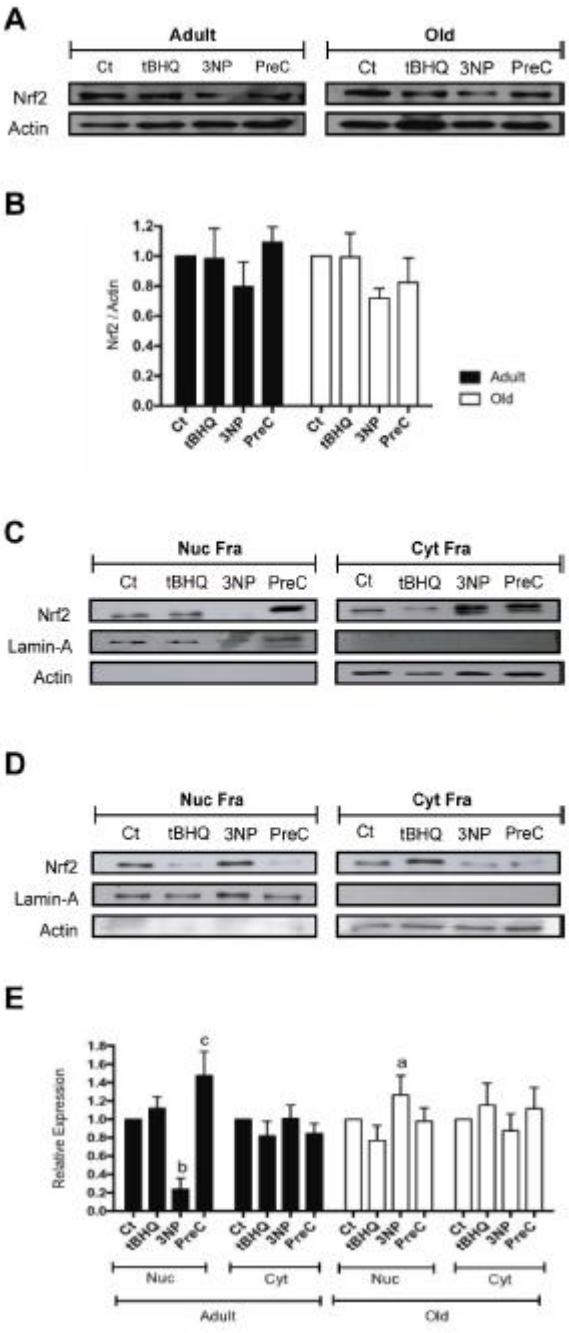


Fig. 6

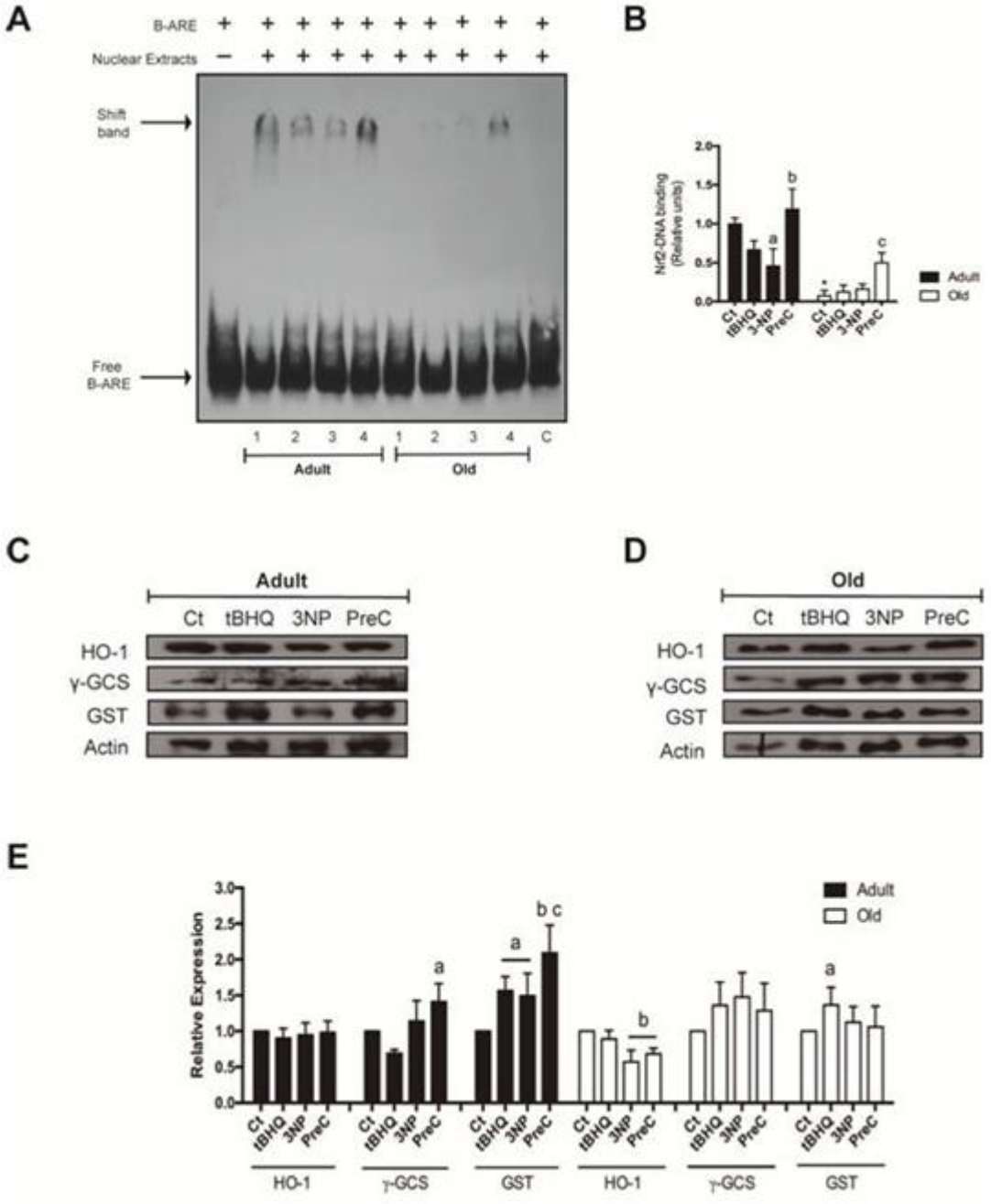
A
B-ARE
Nuclear Extracts
Shift band
Free B-ARE
1 2 3 4 1 2 3 4 C
Adult
Old
B
Nrf2-DNA binding (Relative units)
Ct tBHQ 3-NP PreC Ct tBHQ 3-NP PreC
Adult
Old
C
Adult
Ct tBHQ 3NP PreC
HO-1
γ-GCS
GST
Actin
D
Old
Ct tBHQ 3NP PreC
HO-1
γ-GCS
GST
Actin
E
Relative Expression
Adult
Old
HO-1
γ-GCS
GST
HO-1
γ-GCS
GST

Fig. 7

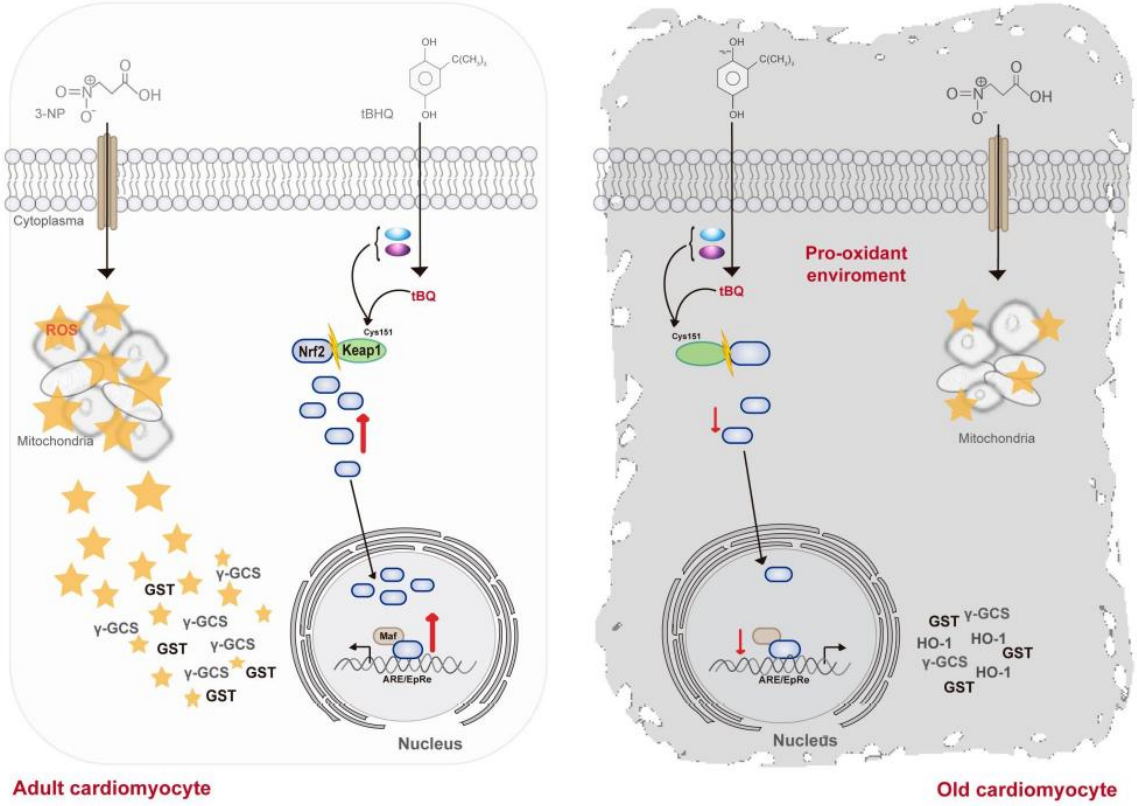


Fig. 8

**Table 1**

| | ADULT | | | | OLD | | | |
|---|---|---|---|---|---|---|---|---|
| **Parameter** | **Ct** | **tBHQ** | **3NP** | **PreC** | **Ct** | **tBHQ** | **3NP** | **PreC** |
| **Body Weight (g)** | 247 ± 8 | 260 ± 13 | 250 ± 9 | 242 ± 19 | **385 ± 33** | 305 ± 31[a] | 318 ± 26[a] | 341 ± 48 |
| **Heart weight (g)** | 1 ± 0.2 | 1 ± 0.1 | 0.9 ± 0.1 | 1 ± 0.1 | **2 ± 0.4** | 1.1 ± 0.1[b] | 1.1 ± 0.1[b] | 1.2 ± 0.1[b] |
| **HW/BW (g/Kg)** | 4 ± 0.4 | 4 ± 0.3 | 3.7 ± 0.6 | 4.3 ± 0.4 | 4.4 ± 1.14 | 3.6 ± 0.4 | 3.4 ± 0.6[a] | 3.7 ± 0.7 |
| **Lung weight (g)** | 2 ± 0.1 | 2 ± 0.3 | 2 ± 0.3 | 2 ± 0.3 | 2.3 ± 0.8 | 2.1 ± 1.0[b] | 1.8 ± 0.5[b] | 2.03 ± 0.4 |
| **LW/BW (g/Kg)** | 9 ± 1 | 8 ± 0.5 | 7 ± 1 | 8.4 ± 1.8 | **6.5 ± 2.9** | 7 ± 3.4 | 5.7 ± 1.0 | 5.9 ±0.9 |
| **IVS (mm)** | 0.2 ± 0.01 | 0.2 ± 0.01 | 0.2 ± 0.01 | 0.18 ± 0.01[b] | 0.2 ± 0.02 | 0.2 ± 0.02 | 0.2 ± 0.01 | 0.2 ± 0.01 |
| **LVDd (mm)** | 5.4 ± 0.3 | 5.1 ± 0.2 | 5.1 0.1 | 5.1 ± 0.06 | 5.2 ± 0.5 | 4.5 ± 0.2 | 4.8 ± 0.4 | 5.2 ± 0.6 |
| **LVSd (mm)** | 3 ± 0.1 | 2.3 ± 0.5 | 2.6 ± 0.1 | 2.7 ± 0.2 | **2.6 ± 0.6** | 1.7 ± 0.4[b] | 2.1 ± 0.5[a] | 2.4 ± 0.5 |
| **EF (%)** | 86 ± 2 | 90 ± 6 | 86 ± 3 | 86 ± 3 | 86 ± 8 | 94 ± 4 | 91 ± 4 | 90 ± 6 |
| **FS (%)** | 48 ± 2 | 59 ± 2 | 49 ± 4 | 48 ± 3 | **53 ± 10** | 62 ± 11 | 56 ± 7 | 54 ± 8 |
| **Heart rate (beats/min)** | 142 ± 6 | 127 ± 10 | 136 ± 2 | 143 ± 16 | **155 ± 22.8** | 137 ± 4.3 | 131 ± 18 | 145 ± 10.7 |
| **Functional parameters** | **(n=4)** | **(n=4)** | **(n=4)** | **(n=3)** | **(n = 6)** | **(n = 3)** | **(n = 3)** | **(n = 3)** |

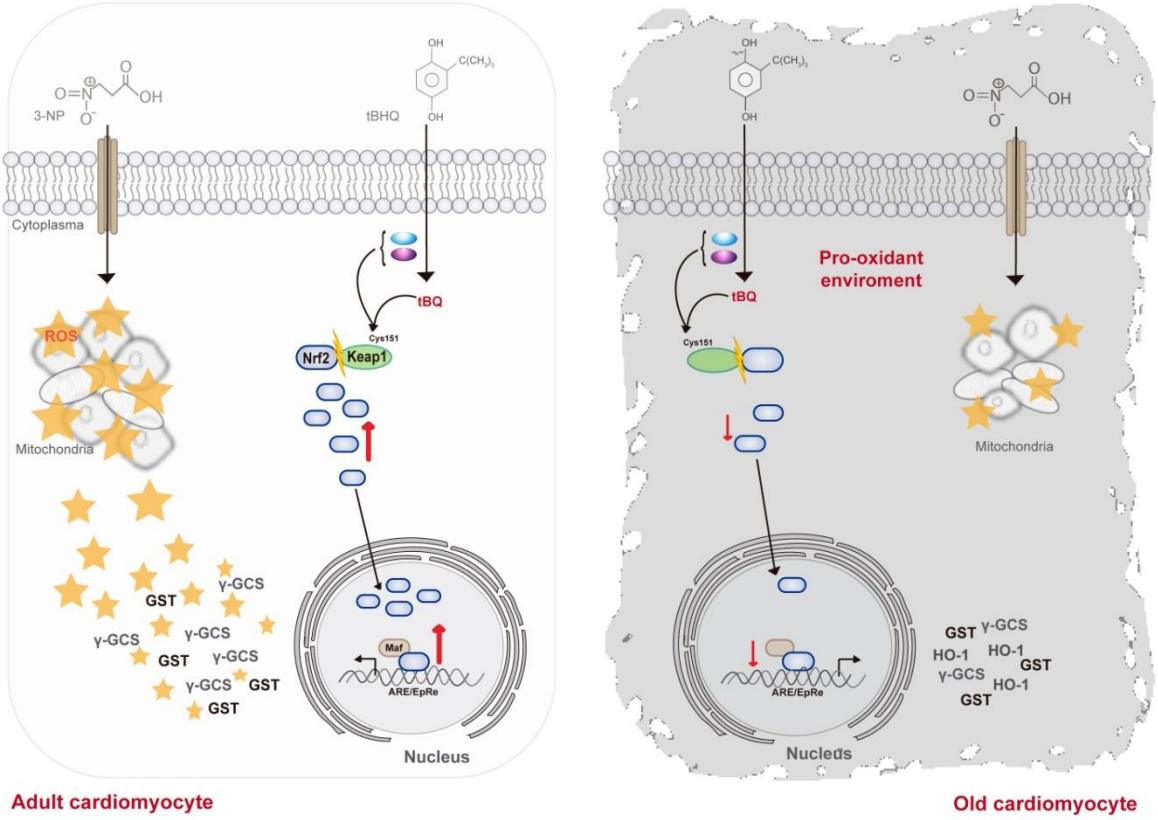


Graphical abstract

**Highlights**

Chronic oxidative stress induces an hormetic response in heart tissue from old rats

3-NP exerts differential effects in cardiac tissue depending on age

The antioxidant response mediated by NRF2 is compromised in old animals